Geological Society of America Bulletin

Structural framework of the Edwards Aquifer recharge zone in south-central Texas

David A. Ferrill, Darrell W. Sims, Deborah J. Waiting, Alan P. Morris, Nathan M. Franklin and Alvin L. Schultz

Geological Society of America Bulletin 2004;116, no. 3-4;407-418
doi: 10.1130/B25174.1

Structural framework of the Edwards Aquifer recharge zone in south-central Texas

David A. Ferrill†
Darrell W. Sims
Deborah J. Waiting
CNWRA, Southwest Research Institute®, San Antonio, Texas, 78238-5166, USA

Alan P. Morris
Department of Earth and Environmental Science, University of Texas, San Antonio, Texas 78249, USA

Nathan M. Franklin
CNWRA, Southwest Research Institute®, San Antonio, Texas, 78238-5166, USA

Alvin L. Schultz
1241 Milam Building, 115 East Travis Street, San Antonio, Texas 78205, USA

ABSTRACT

The Edwards Aquifer, the major source of water for many communities in central Texas, is threatened by population growth and development over its recharge zone. The location of the recharge and confined zones and the flow paths of the aquifer are controlled by the structure of and deformation processes within the Balcones fault system, a major system of predominantly down-to-the-southeast normal faults. We investigate the geologic structure of the Edwards Aquifer to assess the large-scale aquifer architecture, analyze fault offset and stratigraphic juxtaposition relationships, evaluate fault-zone deformation and dissolution and fault-system architecture, and investigate fault-block deformation and scaling of small-scale (intrablock) normal faults. Characterization of fault displacement shows a pattern of aquifer thinning that is likely to influence fault-block communication and flow paths. Flow-path constriction may be exacerbated by increased fault-segment connectivity associated with large fault displacements. Also, increased fault-zone deformation associated with larger-displacement faults is likely to further influence hydrologic properties. Overall, faulting is expected to produce strong permeability anisotropy such that maximum permeability is subhorizontal and parallel to fault-bedding intersections. At all scales, aquifer permeability is either unchanged or enhanced parallel to faults and in many cases decreased perpendicular to faults.

Keywords: Edwards Aquifer, Edwards Group, Balcones fault zone, faults and faulting, normal faults.

INTRODUCTION

The Edwards Aquifer of south-central Texas is composed of Cretaceous limestones of the Edwards Group, consisting of a lower (the Kainer Formation) and upper part (the Person Formation), and the overlying Georgetown Formation (Figs. 1 and 2) (Maclay and Small, 1983; Barker et al., 1994; Maclay, 1995). The Edwards Aquifer is confined beneath younger sedimentary rocks and serves as the primary water source for many communities, including the city of San Antonio (Sharp and Banner, 1997; Hovorka et al., 1998). Aquifer recharge occurs primarily by streamflow loss and infiltration into porous parts of the Edwards Aquifer, where they are exposed within the Balcones fault system, and responds to rainfall in the recharge zone and upslope catchment area. Water in the aquifer locally follows tortuous flow paths controlled by the Balcones fault system. Most recharge of the aquifer occurs along the Balcones fault system where faults, fractures, and dissolution features such as sink holes and caves are major sites for groundwater recharge (Clark, 2000). The high-volume, high flow-rate subsurface flow is also likely dominated by faults, fractures, and solution cavities (Hovorka et al., 1998). Balcones system faults also provide natural discharge sites near New Braunfels and San Marcos and during periods of high rainfall within San Antonio itself (San Pedro and San Antonio Springs; see Fig. 1).

In faulted strata, geologic structures (faults and fractures) exert three controls on aquifer permeability and flow: (1) Faults thin or offset aquifer strata and alter the overall geometry of and communication between fault blocks (Allan, 1989; Maclay, 1989). (2) Fault zones provide barriers to, or pathways for, fluid flow or may form both barriers and pathways (Maclay, 1995; Caine et al., 1996). This fault and fracture conductivity may be influenced by the current stress field and fault activity (Finkbeiner et al., 1997; Ferrill et al., 1999b). (3) Fault-block deformation by formation of small faults and fractures leads to permeability anisotropy (Mayer and Sharp, 1998; Ferrill et al., 2000).

In addition to the three general controls detailed above, carbonate rock layers like those of the Edwards Aquifer are subject to localized groundwater flow and associated limestone dissolution (Deike, 1990). Such dissolution may enhance the permeability of fault and fracture systems, including solution enlargement at scales from individual fractures to cave networks consisting of fissures, angular passages, and fracture-controlled net-

†E-mail: dferrill@swri.org.

GSA Bulletin; March/April 2004; v. 116; no. 3/4; p. 407–418; doi: 10.1130/B25174.1; 8 figures; 1 table.

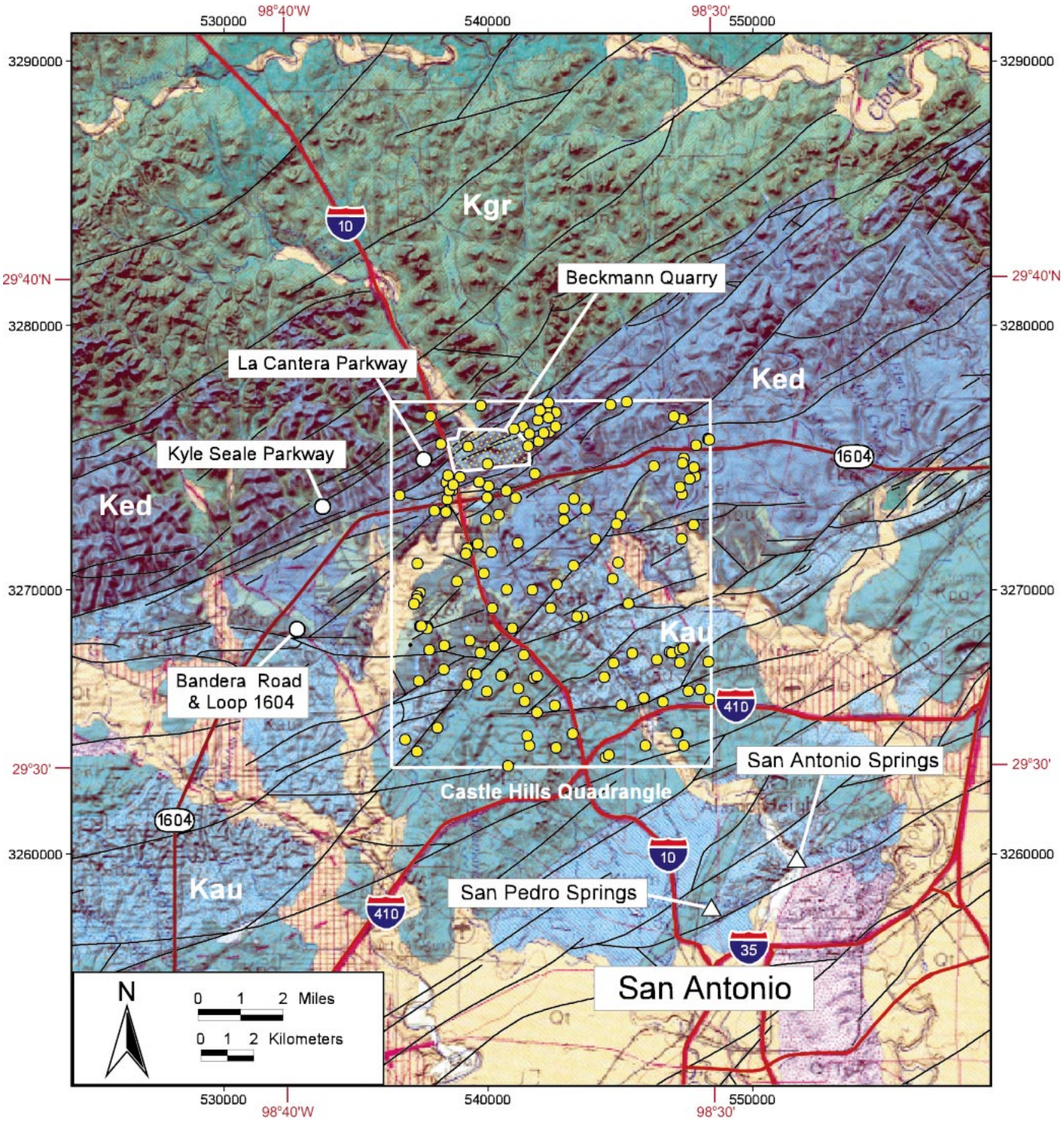

Figure 1. Location map of a part of the Balcones fault system and Edwards Aquifer recharge zone in northwest San Antonio and Texas Hill Country. Geologic map of Barnes (1983) is draped over the hill-shaded digital elevation model. White box shows the location of the Castle Hills 7.5′ quadrangle (area of Fig. 3). Fault traces (black lines) are from Collins and Hovorka (1997). Yellow dots are locations of well-bore data used in construction of geologic framework model. Cretaceous geologic units: Kau—Austin Group; Ked—Edwards Group; Kgr—Glen Rose Group. Map coordinates shown are UTM, zone 14 (black numbers) and Geographic Coordinate System (red numbers).

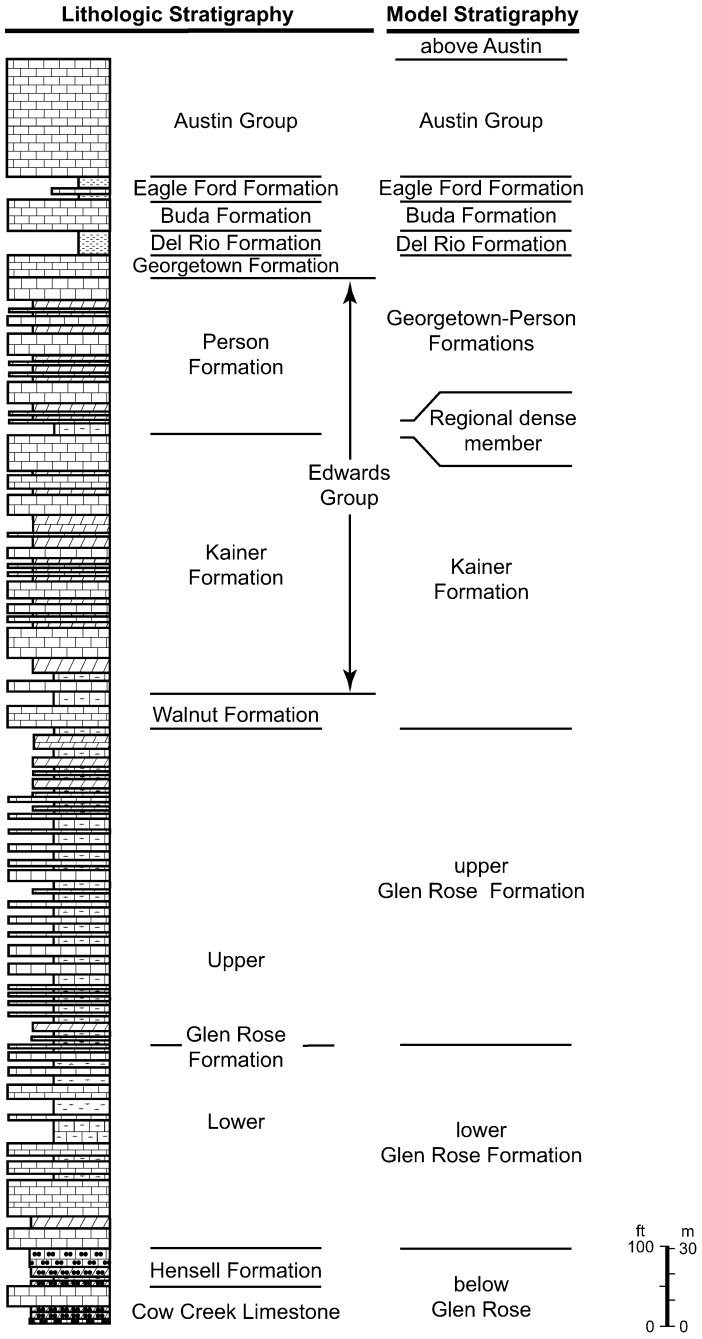

Figure 2. Stratigraphic column showing relationship between lithologic stratigraphy and model stratigraphy. Stratigraphic column is after Collins (2000). Note that prominent shale units (Eagle Ford Formation, Del Rio Formation) separate the limestones of the Austin Group, Buda Formation, and Edwards Aquifer strata. The Glen Rose Formation is considered to be the lower confining unit. Argillaceous (clay-rich) layers in the Glen Rose are not as thick or as clay rich as those of the Eagle Ford or Del Rio Formations.

works of passages (Palmer, 1991; Loucks, 1999). Alignment of linear cave segments and cave networks with fracture patterns and direct observation that caves are associated with faults and fractures indicate fault and fracture control on caves in the Edwards Aquifer recharge zone (Wermund and Cepeda, 1977; Wermund et al., 1978; Kastning, 1981; Clark, 2000; Ferrill and Morris, 2003).

In this paper, we present results of structural investigations conducted in the Edwards Aquifer recharge zone and Balcones fault system near San Antonio, Texas, as well as supporting examples of well-exposed and structurally similar examples from analogous faulted limestones in west Texas. These investigations span the range of structural scales: (1) three-dimensional geologic framework modeling to constrain large-scale aquifer architecture in the study area, (2) analysis of fault offset and stratigraphic juxtaposition, (3) analysis of fault-zone deformation and dissolution and fault-system architecture, and (4) examination of fault-block deformation and small-scale (intrablock) normal faults. The result is a systematic overview of fault-system characteristics and deformation mechanisms that are likely to influence recharge into and flow within the Edwards Aquifer.

CHARACTERIZATION OF AQUIFER ARCHITECTURE

The Balcones fault system is a broad en echelon system of mostly southeast-dipping normal faults that formed during the middle to late Tertiary (Foley, 1926; Murray, 1961; Young, 1972). The arcuate zone trends east-northeast and spans much of central Texas. The 25–30-km-wide Balcones fault system has a maximum displacement of 366 m (Weeks, 1945) and defines the transition from structurally stable flat-lying rocks of the Texas craton to gently coastward-dipping sedimentary deposits of the subsiding Gulf of Mexico. At the margin of the Texas Hill Country northwest of San Antonio, exposures in Cretaceous platform carbonates include the Edwards Group, a succession of carbonate strata deposited along the margin between the Central Texas platform and the ancestral Gulf of Mexico (Fig. 1) (Rose, 1972). Offset of carbonate strata across the Balcones fault system resulted in a broad, weathered escarpment of vegetated limestone hills rising from the predominantly clastic coastal plains to the uplands of the Texas craton. Within the fault system, the dip of bedding varies from gentle coastward dips to nearly horizontal; a few hanging-wall beds locally dip northward into some faults. Growth faulting is not apparent in outcrop along the fault zone. Faulting has been interpreted as being rooted in the deeply buried foreland-basin sedimentary rocks of the Ouachita orogeny (Murray, 1956).

We constructed a three-dimensional digital geologic framework model of a part of the recharge zone and confined zone of the Edwards Aquifer by using EarthVision® 6.1 (Figs. 2 and 3A; Dynamic Graphics®, 2001). The model was constructed to represent the faulted Edwards Aquifer and confining strata and to

elucidate potential structural controls on recharge, groundwater flow, and transmissivity within the aquifer. The model covers the area outlined by the U.S. Geological Survey (USGS) 7.5′, 1:24,000 Castle Hills Quadrangle. The upper boundary of the model is the topographic surface (maximum elevation 450 m). The lower boundary is at a depth of 100 m below mean sea level. USGS 30 m digital elevation data in DEM (digital elevation model) format were used to construct the topographic surface.

Eleven stratigraphic horizons present in outcrop or in the subsurface are represented in the model volume (Fig. 2). Stratigraphic horizons were selected to define the principal hydrogeologic units and for characteristics that allow for their recognition in outcrop or geophysical logs. The model units include aquifer strata and the upper and lower confining strata. Model horizon designations, from oldest to youngest, are ''below Glen Rose,'' ''lower Glen Rose Formation,'' ''upper Glen Rose Formation,'' ''Kainer Formation,'' ''regional dense member,'' ''Georgetown-Person Formations,'' ''Del Rio Formation,'' ''Buda Formation,'' ''Eagle Ford Formation,'' ''Austin Group,'' and ''above Austin.'' The Walnut Formation (Collins, 2000) is included in our model as the basal nodular member of the Kainer Formation (Maclay and Small, 1984).

Structure in the model is constrained by using maps and cross sections (Arnow, 1963; Reeves, 1972; Small and Hanson, 1994; Hanson and Small, 1995; Groschen, 1996; Stein and Ozuna, 1996; Collins and Hovorka, 1997; Collins, 2000), results from field investigations, and geophysical well-log interpretations. Because published geologic and hydrogeologic maps of the Balcones escarpment do not show uniform interpretations of fault traces or surface outcrops, we formulated a set of criteria by which to reconcile the different interpretations. Faults from published maps are generally included in the model where (1) the fault is present and congruent in all interpretations, (2) the fault is present on one or more maps and is required to reconcile outcrop or subsurface data, (3) the fault shows vertical offset greater than ~15 m (50 ft), or (4) the fault is present on one or more maps and is geometrically reasonable with respect to the fault system. The selection of 15 m as the threshold vertical displacement is based on the ambiguity and inconsistency in regional mapping of faults with offsets smaller than this, particularly where mapped faults are based on unclear field and well-bore data. Faults with ≤15 m vertical displacement reduce the thickness of the Edwards Aquifer

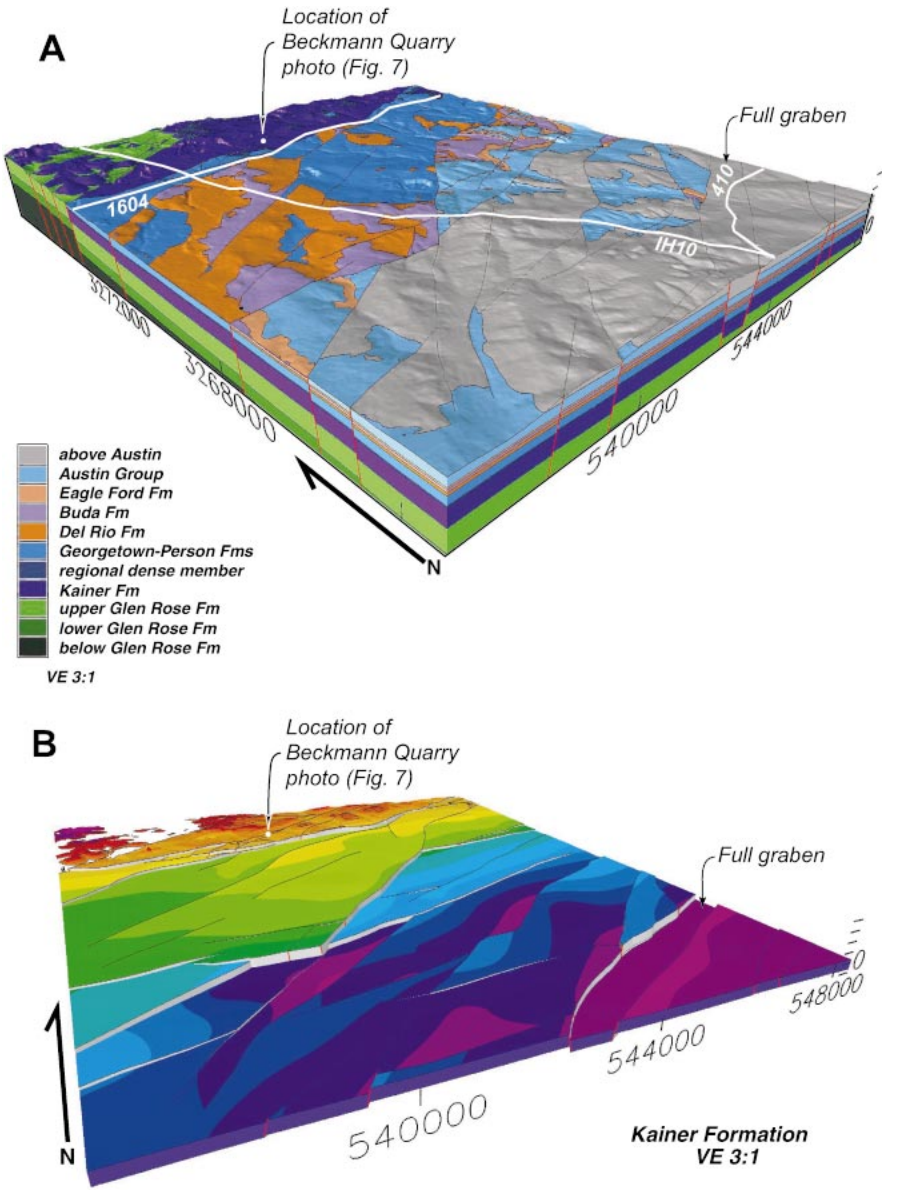

Figure 3. (A) Oblique view of geologic framework model. Coordinates are UTM zone 14. Look direction is northeast. Illumination from southwest. (B) Color-contoured Kainer layer in the Castle Hills Quadrangle model area. Warm colors (orange, red) represent higher elevations; cooler colors (purple, blue) represent lower elevations.

(mean thickness = 153 m) by ≤10%, and therefore, are less likely than larger faults to strongly influence groundwater flow. Faults from published maps are generally excluded where (1) maximum vertical displacement is less than 15 m, (2) the fault is in conflict with outcrop or subsurface data, or (3) the fault is not required to accommodate horizon or fault-system geometry. The selection of faults was refined and supported by published (Small, 1984, 1985) and new interpretations of geophysical well logs.

Few data are available to constrain subsurface geometry of individual faults. Some fault systems are exposed in quarries or roadcuts. Where present, slip indicators on these exposed fault surfaces show predominantly normal dip-slip displacement. In the model, fault dip directions were constrained by assuming that offsets of stratigraphic horizons resulted from normal dip-slip displacement. Dip angles were constrained by measuring small faults exposed in roadcut exposures of the Edwards Group and Glen Rose Formation. An average dip for each of these units was computed on the basis of field measurements of exposed

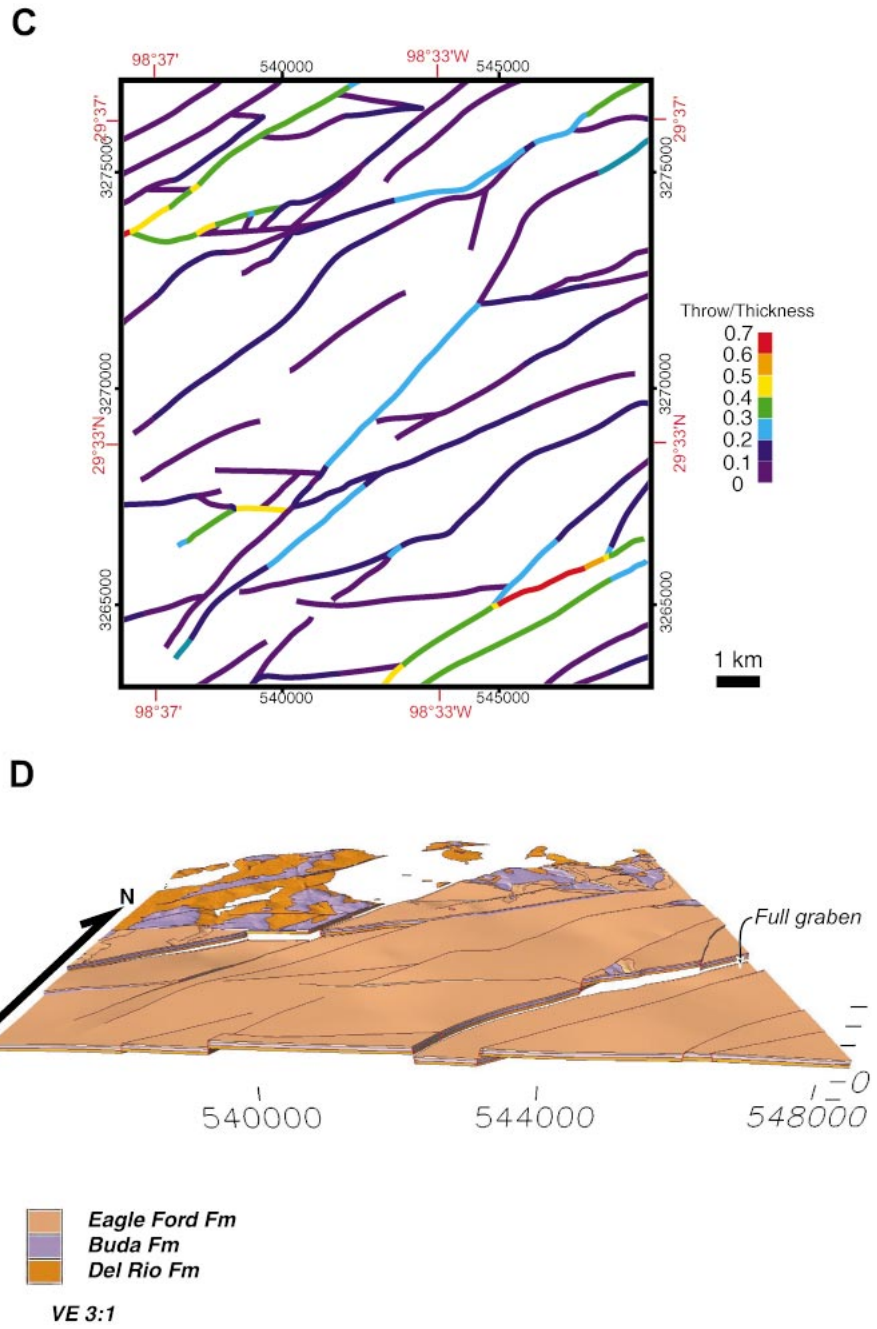

Figure 3. (*Continued*) (C) Map of faults within the three-dimensional model area color-coded according to throw/mean thickness ratio. Thickness of Edwards Aquifer is taken to be 153 m (Table 1). Map coordinates in red are in Geographic Coordinate System. (D) Del Rio, Buda, and Eagle Ford Formations in the model. Look direction is north; illumination from southwest.

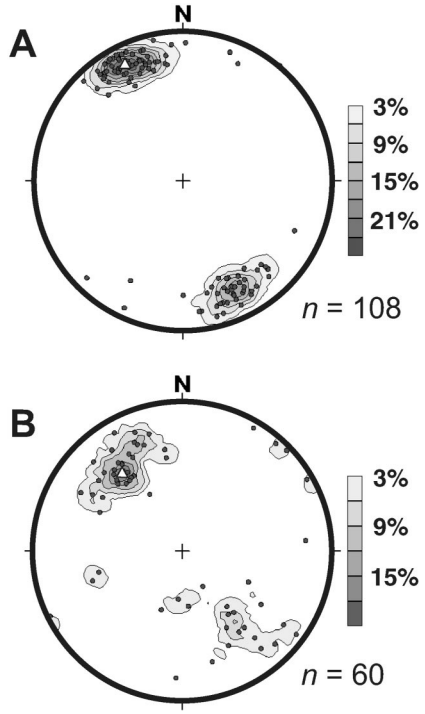

Figure 4. Lower-hemisphere, equal-area stereographic projection of poles to fault planes. (A) Poles to 108 fault planes measured in exposures of the Edwards Group, showing average dip magnitude of 75°. Data were collected along La Cantera Parkway (see Fig. 1 for location). (B) Poles to 60 fault planes measured in exposures of the Glen Rose Formation, showing average dip magnitude of 60°. Data were collected along U.S. Highway 281, north of Bulverde, Texas.

faults (Fig. 4). In the model, faults with surface traces in the Edwards Group have a uniform dip of 75°, and those with surface traces in the Glen Rose Formation have a uniform dip of 60°. Field observations of the fault systems exposed in quarry walls and roadcuts indicate that displacement is commonly distributed across a zone of smaller-displacement faults rather than concentrated in a single large fault. In most cases, individual faults are below the scale of our model, and fault zones are represented as single fault surfaces.

Regional dip of bedding in the area is gentle (<1°) and toward the southeast. Tilting of faulted blocks is generally mild to undetectable, with the occasional exception of localized low-angle antithetic dip (opposite direction to fault dip) of bedding (Collins, 1993) or synthetic dip (in the same direction as the fault dip) seen in monoclines above fault tips and in faulted monoclines. Steep bedding dip associated with relay ramps is not generally observed (Collins, 1993).

Our three-dimensional geologic framework model of the geology of the Castle Hills Quadrangle was constructed by using a reference-isochore method, in which a reference horizon is constructed from outcrop, fault, and subsurface data. In our model, the top of the upper unit of the Glen Rose Formation serves as the reference horizon. The upper Glen Rose extends across the entire model volume and is widely and well constrained by outcrop and well-bore data. Upon completion of the reference horizon, model horizons above and be-

TABLE 1. VARIATION IN MODEL HORIZON THICKNESS

Model horizon name	Min. thickness (m)	Max. thickness (m)	Mean thickness (m)
Above Austin	N.A.†	N.A.	N.A.
Austin Group	25.0‡	60.8	37.1
Eagle Ford Formation	4.6	11.6	7.6
Buda Formation	12.5	17.2	15.7
Del Rio Formation	11.0	19.8	14.7
Georgetown-Person Formations	38.5	71.3	51.2
Regional dense member (Person Formation)	N.A.	N.A.	7.0
Kainer Formation	79.8	102.6	95.0
Upper Glen Rose Formation	N.A.	N.A.	121.9
Lower Glen Rose Formation	N.A.	N.A.	76.2
Below Glen Rose	N.A.	N.A.	N.A.

† Not applicable.
‡ Eroded thickness.

low the upper Glen Rose reference horizon are projected by using stratal thickness. Thickness variations are reported for each of the lithostratigraphic horizons represented in the model (Arnow, 1963; Maclay and Rettman, 1972; Maclay and Small, 1976, 1983; Shaw, 1978; Small, 1984, 1985; Barker et al., 1994; Collins, 2000). Sufficient data are available to incorporate local thickness variation for 6 of the 11 model horizons (Table 1). For each of these 6 horizons, thickness is calculated from wellbore thickness data through the use of minimum tension gridding, by which surface curvature is distributed by nonlinear interpolation between grid nodes. Constant-thickness values from the geologic map by Collins (2000) were used for the lower Glen Rose Formation, upper Glen Rose Formation, and regional dense member model horizons (Table 1) for which lateral thickness data were not available.

The 11 horizons in our geologic framework model are offset by 50 faults. Dominant fault-trace orientation is northeast-southwest, and dip and displacement are predominantly down to the southeast. Most faults intersect with other faults at one or both ends or are cut by the model boundaries. Vertical offset (throw) ranges from zero to a maximum of ~129 m on a single fault, and lateral displacement gradients are generally small. Fault blocks are elongate in map view, with the long axis oriented northeast-southwest, and block tilting is gentle. Half grabens are dominant, but full grabens are also present (Figs. 3B, 3D). Maximum fault offset is concentrated along three fault systems (Figs. 3B–3D). One of these systems forms the northern boundary of the aquifer recharge zone, where rocks of the Edwards Group are juxtaposed against rocks of the Glen Rose Formation.

FAULT JUXTAPOSITION

With increasing fault displacement, original hydraulic communication pathways are diminished or broken and new pathways may be formed. Simple geometric juxtaposition analysis as described by Allan (1989) assumes that the fault zone has no particular properties that cause it to differ from unfaulted host rock. Maclay and Small (1983; also Maclay, 1989) used a similar approach to analyze juxtaposition of permeable zones and relatively impermeable zones in the Edwards Aquifer and coined the term ''barrier fault'' for faults across which hydraulic connection is partly or completely lost owing to fault displacement (aquifer thinning).

Viewing the Kainer model layer, the lower two-thirds of the Edwards Aquifer (Table 1, Fig. 2), in three dimensions, reveals important juxtaposition characteristics of the Edwards Aquifer in the model area (Fig. 3B). The throw along some fault segments is greater than the thickness of the Kainer; hence the aquifer is structurally thinned by 67% in these locations (throw/thickness ratio = 0.67; Fig. 3C). In locations of significant aquifer thinning by fault displacement, flow diversion can cause the local water table to fluctuate from fault block to fault block (e.g., Maclay and Small, 1983). In these locations, the full thickness of the Kainer in the fault hanging wall is juxtaposed against the upper Glen Rose and, in one case, the top of the Lower Glen Rose. This juxtaposition is important for assessment of potential groundwater communication between the Trinity Aquifer (Glen Rose) and the Edwards Aquifer. The largest individual faults form a pronounced escarpment along their strike trend (Balcones Escarpment in Fig. 5). Displacement on these faults is sufficient (>150 m) to completely offset the Edwards Aquifer from itself by juxtaposing older and younger strata across the fault.

Viewing the upper confining layer (Del Rio, Buda, and Eagle Ford Formations) shows that this relatively thin stratigraphic sequence is in many places offset by more than the mean thickness of the sequence (38 m; see Table 1; Fig. 3D). The Buda Formation and Austin Group in fault hanging walls are, in some cases, juxtaposed against the Edwards Aquifer in the fault footwall, providing the potential for recharge of the Edwards Aquifer from the Buda Formation or Austin Group. This recharge geometry is further complicated by the general south or southeast regional dip (e.g., Fig. 3B). There are several locations in the model where either south-dipping layers intersect north-dipping faults or where relatively large displacement gradients on faults have overcome regional dip to produce northeastward dip. Therefore, based on the juxtaposition geometry, it is conceivable that limestones in fault hanging-wall blocks could locally recharge the Edwards in footwall blocks in the subsurface. However, it is difficult to elucidate potential recharge of the Edwards just from analyzing strata. The potential for distributed deformation or ''smearing'' of Del Rio Formation clay along faults suggests that simple juxtaposition analyses may overestimate actual hydrologic communication across faults.

FAULT-ZONE PROPERTIES, CONTINUITY, AND DISTRIBUTION

Fault-System Architecture

Slip-tendency analysis (e.g., Morris et al., 1996; Ferrill et al., 1999b) of the Balcones fault system, applying a normal-faulting stress system based on 1 km of water-saturated overburden with an average rock density of 2.7 g/cm^3 and with an extension direction of 145° (σ_1 = vertical, 17 MPa; σ_2 = azimuth 055°, 11 MPa; σ_3 = azimuth 145°, 5 MPa), indicates that most of the major faults would have exhibited a high slip tendency in a regionally uniform stress field (see rose diagram in Fig. 5). The obliquity of fault strike to fault-system trend reflects an en echelon fault system. In the early stages of the development of en echelon normal-fault systems, fault-block connectivity remains high, whereas fault connectivity remains low. With progressive extension, faults link by intersection of curved fault tips or the formation of connecting faults, and fault-block connectivity declines as fault connectivity increases (Ferrill et al., 1999a; Ferrill and Morris, 2001). Through the San Antonio area, displacement is distributed across a 12-km-wide displacement transfer system or relay ramp (Collins and Hovorka, 1997) (Fig. 5).

In a mechanically layered stratigraphic sequence, vertical displacement gradients on normal faults may be pronounced and are

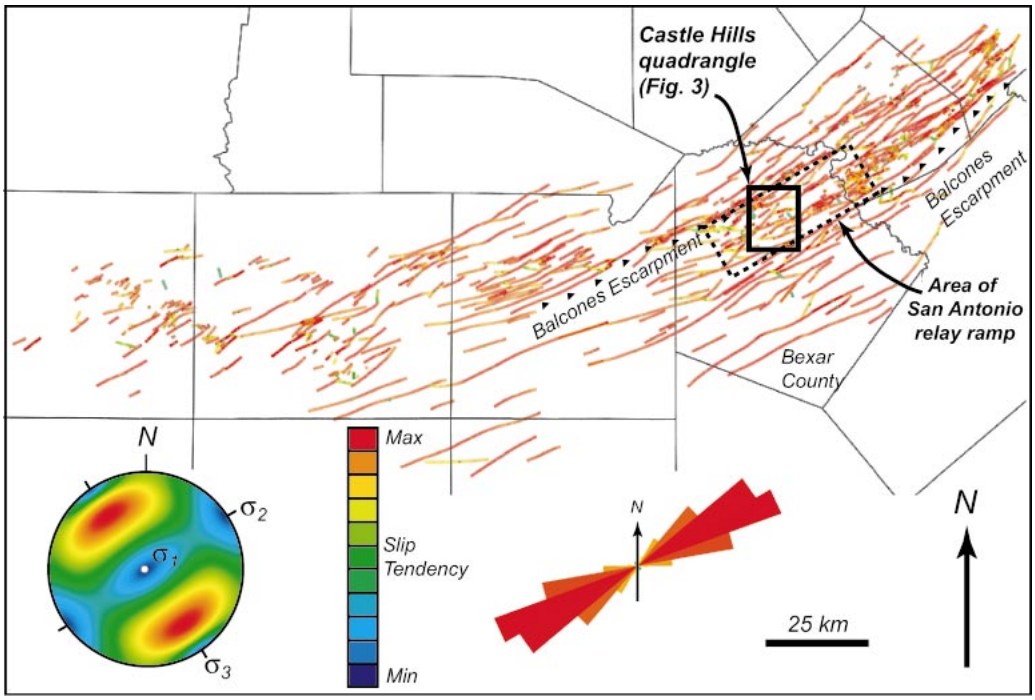

Figure 5. Map of the Balcones fault system in the San Antonio area with fault traces colored according to their slip tendencies. Slip-tendency analysis was performed by using 3Dstress™, version 1.3.3 (Southwest Research Institute [SwRI®], 2000), based on mapped faults of Collins and Hovorka (1997). See text for further details.

largely controlled by stratigraphy. A mechanically weak layer within a relatively strong deforming stratigraphic section can arrest fault-tip propagation and result in monoclinal folding prior to fault breakthrough (Withjack et al., 1990). The most extreme case of mechanical stratigraphy contrast associated with the Edwards Aquifer is at the contact between the top of the Edwards Aquifer (153 m mean thickness, well-bedded crystalline limestone) and the Del Rio Formation (11–20 m thickness, primarily clay-rich shale with thinly bedded limestone). Equivalents of these rocks are exceptionally well exposed in the Sierra del Carmen mountain range of west Texas where the resistant (ridge-forming) Cretaceous Santa Elena Limestone has largely been exhumed by erosion of the overlying Del Rio Formation (Maxwell et al., 1967; Moustafa, 1988). The Sierra del Carmen range provides excellent examples of the geometry and deformation processes likely to occur in the Edwards Aquifer and recharge zone. In Big Brushy Canyon, the Santa Elena Limestone (equivalent in age and lithology to the Edwards) is displaced by at least 30 m on a north-northwest–trending, down-to-the-east normal fault. The overlying Del Rio Formation is not completely cut by the fault, but is dramatically thinned over the fault tip (Fig. 6), and above the Del Rio Formation is the Buda Formation, which forms a fault-propagation monocline over the fault (Fig. 6). Further displacement on the normal fault in this exposure would have breached the monocline. Even in the present-day configuration, the Buda Formation has been displaced to a level below the top of the Santa Elena Limestone across the fault. The two limestones, however, are not in physical contact with one another. The Del Rio Formation has been folded and smeared along the fault, and this smear along with calcite mineralization in the fault zone is likely to produce a barrier to across-fault fluid communication.

The overall en echelon geometry of the Balcones fault system would, in general, be expected to produce poorly connected faults and result in well-connected layers early in fault-system development. Competing with this is the apparent rapid lateral propagation of fault segments with respect to displacement accumulation (based on general absence of large lateral-displacement gradients) at least within stronger mechanical layers. This rapid propagation would have resulted in early interconnection of faults and loss of stratigraphic communication pathways. Field observations show that vertical connectivity is controlled by mechanical stratigraphy and that weak mechanical layers are capable of arresting fault-tip propagation at a variety of scales.

Fault-Zone Deformation

Fault-zone deformation includes mechanical and chemical alteration of rock properties, both in the principal displacement zone (fault core) and the zone of less intense fault damage (damage zone), developed adjacent to the fault core (Caine et al., 1996). Normal faults in stratified rocks commonly have dip changes that can form by compaction or interaction between different fault segments during fault propagation and displacement accumulation (Ferrill et al., 2000). In addition, faults are initiated with failure angles that are controlled by rock mechanical properties and effective stresses at the time of failure (e.g., Walsh and Watterson, 1988; Ferrill and Morris, 2003). This effect is accentuated when failure occurs at shallow depths where differential effective stress is low and minimum principal effective stress is likely to be near zero or tensile (cf. Ferrill and Morris, 2003). Under these conditions, rocks fail in several modes and with variable failure angles. Changes in failure angle vertically through a mechanically layered rock sequence produce faults with refracted geometries defined by steeper dips in competent beds and gentler dips in less competent beds. Where subsequent slip parallels the more gently dipping segments, the steeper segments dilate (Ferrill and Morris, 2003). Di-

latant segments along faults within carbonate rocks of the Cretaceous Edwards Group have been enlarged by groundwater flow and are important permeability and shallow groundwater-infiltration pathways (Ferrill and Morris, 2003).

One fault in Beckmann Quarry has been exhumed and is exposed in exceptional detail. This fault is exposed along strike for a distance of ~100 m and vertically in three-dimensional exposure for a height of 15 m (fault A, Fig. 7). The footwall of the fault over most of its exposure consists of the basal nodular member of the Kainer Formation. The top of the exposure was at a preexcavation depth of ~50 m (Fig. 7). The fault is part of an en echelon array. Although most faults in the area are mapped with remarkable consistency of orientation, this fault changes strike by 80° at its southwestern end, loses displacement, and tips as it intersects with another en echelon fault (fault B in Fig. 7; also cf. Ferrill et al., 1999a). Fault A is vertically segmented in the tip region, with offset distance between the vertically overlapping segments on the order of tens of centimeters. The footwall fault surface is characterized by visible layers and bedding-plane partings locally obscured by patches of fault rock (cataclastic host-rock material and precipitated coarsely crystalline calcite, locally impregnated with devolatilized oil) and corrugations, grooves, and striations indicating down-dip fault slip.

The fault plane exposed in Beckmann Quarry is within the present-day unsaturated zone. Dissolution features on the fault plane consist of tubes and cavities, some of which have been filled or partly filled by terra rosa clay, a residue from dissolution of limestone. These dissolution features are more than 50 m below the pre-excavation ground surface and, on the basis of their predominantly down-dip long-axis orientations, are indicative of down-dip water movement. Flow paths are in some cases discontinuous or intermittently present down the fault plane in the visible footwall. This apparent lack of continuity suggests that the flow paths in three dimensions crossed the fault core from footwall to hanging wall and back.

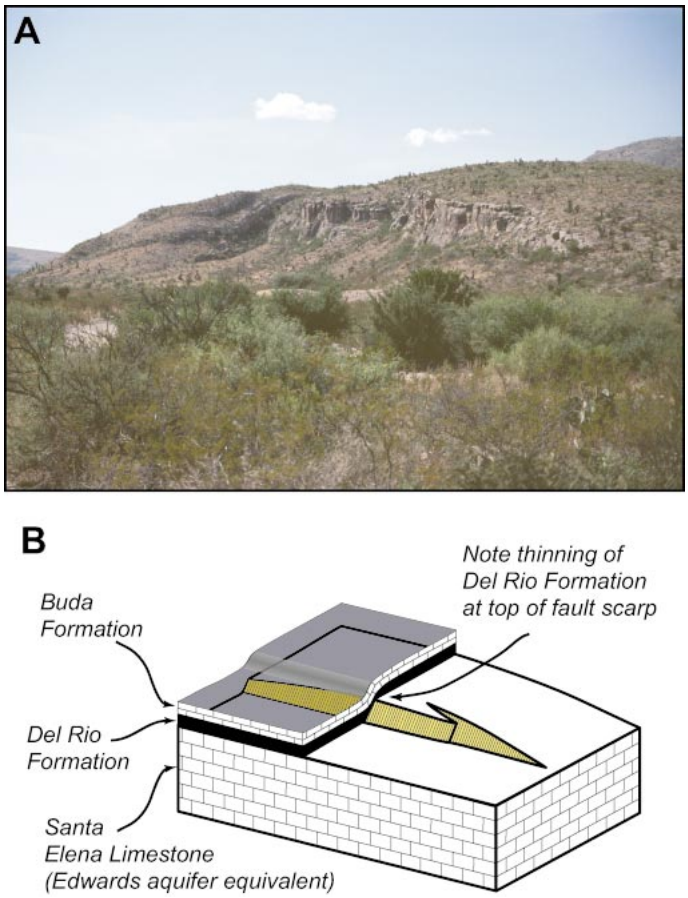

Figure 6. (A) Field photograph of Big Brushy Canyon monocline (view is to the southwest). (B) Block diagram illustrating the Big Brushy Canyon monocline. This monocline is located in the northeastern part of the Black Gap wildlife management area in the Sierra del Carmen mountain range of west Texas. Note that the displacement that produced the prominent fault scarp in the Santa Elena Limestone (equivalent of upper part of Edwards Aquifer) is accommodated upward by folding of the Buda Formation. The Del Rio Formation arrests upward fault tip propagation, resulting in the formation of a fault-propagation fold in the overlying Buda Formation. The Del Rio Formation clay layer is attenuated and may coat the fault surface to form a barrier between the Buda Formation and Santa Elena Limestone, even in situations where the two limestones are juxtaposed by faulting.

FAULT-BLOCK DEFORMATION

The magnitude of deformation and the orientations of small faults and fractures within fault blocks are major contributors to permeability anisotropy within fault blocks. The evolution of extensional fault systems is characterized by nucleation and growth of numerous faults, which then become linked into a network of faults (e.g., Dawers and Anders, 1995; Ferrill et al., 1999a). During development of extensional-fault systems, faults typically have displacement gradients along their lengths, which lead to deformation within adjacent fault blocks (Ferrill and Morris, 2001).

Faults with displacements of millimeters to <10 m in the Edwards Aquifer recharge zone most commonly parallel the regional fault trend. Although faults with the regional southeast dip are dominant, conjugate faults dipping to the northwest are also very common (Fig. 4A; Ferrill et al., 2000). Our observations of ~5 km of exposure in quarries and roadcuts in Edwards Aquifer strata indicate that systems of small faults are heterogeneously developed within fault blocks. Scan-line studies in accessible roadcut exposures (two localities near the northwest corner of the Castle Hills Quadrangle in northwest San Antonio) within the Kainer Formation demonstrate this heterogeneity. In a roadcut exposure along Kyle Seale Parkway, extension by small-scale faults is 0.1%, and fault intensity is 0.04 faults per meter over an extension-parallel distance of 198 m (Fig. 1). In a nearby roadcut exposure along La Cantera Parkway adjacent to a mapped fault, extension by small-scale faults is 7.6%, and fault intensity is 1.16 faults per meter over an extension-parallel distance of 93 m (Fig. 1). These two examples represent the end members of fault-intensity variation

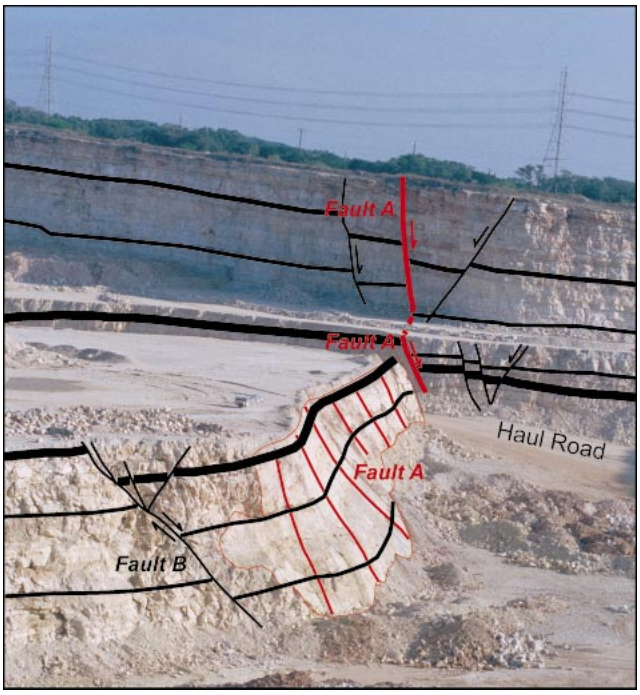

Figure 7. Field photograph from top of quarry wall, looking northeast across Beckmann Quarry, illustrates a three-dimensional exposure of a fault. Quarry is ~65 m deep. See text for details.

that we have observed in Edwards Aquifer strata. In the case of low fault intensity (Kyle Seale Parkway), faulting must have little effect on either permeability magnitude or anisotropy. In the case of higher fault intensity (e.g., La Cantera Parkway), faulting is expected to influence permeability and produce strong permeability anisotropy such that maximum permeability is approximately parallel to fault strike and/or to fault/fault and fault/bedding intersections as described by Ferrill et al. (1999b, 2000) and Ferrill and Morris (2003). From observations of dissolution features along small faults in the Edwards, it appears that faults commonly increase permeability. In some cases, however, fault-zone processes of grain-scale deformation, precipitation, and accumulation of devolatilized oil may locally occlude porosity and reduce permeability. The development of permeability anisotropy will occur in either case (Ferrill et al., 2000). We conclude that zones of high fault intensity are generally within 100 m (perpendicular to strike) of a large-displacement (maximum displacement >10 m) fault.

DISCUSSION

Geologic structures in the Edwards Aquifer influence permeability architecture at a range of scales. At the largest scale, the influence of faults and fractures on the aquifer could be described by using a single permeability tensor. However, at the scale of individual recharge features, flow conduits, and wells in the Edwards Aquifer, significant heterogeneity is observed. Here we consider the scale range from regional flow models down to that of individual recharge features, flow conduits, and wells.

Structural control on permeability architecture is subdivided into three components, as depicted in Figure 8A. At the largest scale, major faults of the Balcones fault system control the overall geometry of the aquifer, including its position at the ground surface (recharge zone), dip magnitude and direction, and position of the aquifer in the subsurface. Major faults produce tilting of fault blocks and locally thin the aquifer to some fraction of its original thickness. Thus, aquifer communication is decreased in directions perpendicular to the fault strike because of aquifer thinning. Fault zones themselves generally have reduced permeability perpendicular to the zones and increased permeability parallel to the zones, providing for vertical and lateral flow within faults. In sum, faults may serve as local flow conduits. Smaller faults and extension fractures within fault blocks produce permeability anisotropy within the blocks. Fault-block deformation in the form of heterogeneous, small-scale faulting and extension fracturing is observed within the Edwards Aquifer. High intensities of small faults occur close to large faults (within ~100 m).

Aquifers (and hydrocarbon reservoirs) can be qualitatively classified within a ternary system on the basis of these three structural controls on permeability architecture (Fig. 8B). The exact role of faults and fractures will vary with rock type, structural setting, deformation conditions, and geochemical activity. In the Edwards Aquifer, the role of major faults for geometry and thinning of the aquifer has been identified (Maclay and Small, 1983; Hovorka et al., 1998; Collins, 2000), as has the importance of individual faults as infiltration and subsurface flow pathways (Clark, 2000; Ferrill and Morris, 2003). The role of fault-block deformation in the Edwards Aquifer is variable and is controlled primarily by structural position (Fig. 8B), especially proximity to large (>10 m maximum displacement) faults.

An important question with respect to the Edwards Aquifer recharge zone, and related subsurface groundwater flow in the confined Edwards Aquifer, is whether subsurface flow occurs (1) across faults within the Edwards Aquifer, (2) between the Edwards Aquifer, Buda Formation, and Austin Chalk higher in the stratigraphic section, and/or (3) between the Edwards Aquifer and the Glen Rose Formation below (Trinity Aquifer). Water that infiltrates in other stratigraphic units may be capable of flowing laterally into the Edwards Aquifer. This potential for subsurface aquifer communication is important because it influences the amount and distribution of areas that provide recharge to the Edwards Aquifer, thereby effectively expanding the recharge zone. In addition, communication between aquifers could mean increased threat for contaminant migration into the Edwards Aquifer from other aquifers (Trinity Aquifer).

Faults that juxtapose the Edwards Aquifer with itself are not likely to be effective barriers to across-fault aquifer communication, because the Edwards Aquifer stratigraphic section does not contain significant clay-rich sealing layers. Field observations, in particular the common occurrence of dissolution enlargement of faults, suggest that fault-zone deformation processes in these limestones more commonly enhance rather than reduce permeability. Structural thinning of the aquifer by normal faults does, however, constrict flow (communication) pathways (Maclay and Small, 1983). Continuous monitoring of water-table elevations in the unconfined Edwards Aquifer in the recharge zone shows that water levels do change across some faults (Steve Johnson,

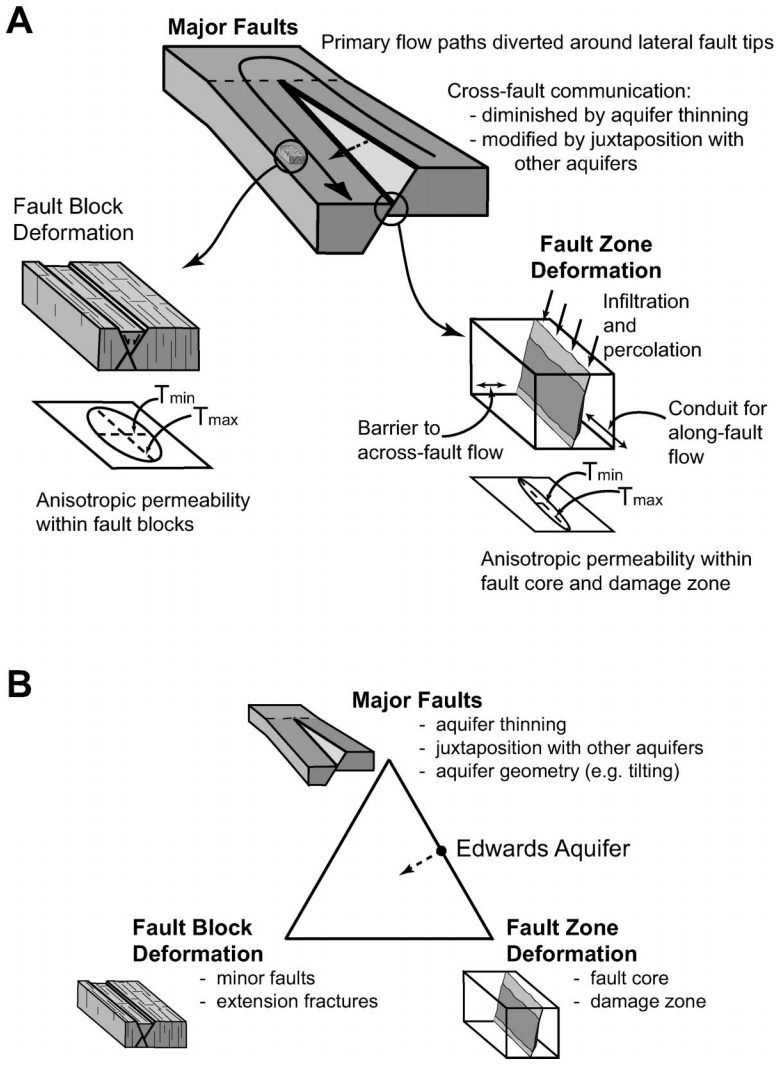

Figure 8. Structural controls on permeability architecture. (A) Schematic illustration of interplay between the three major elements of structural control on the Edwards Aquifer. T_{min} and T_{max} refer to minimum and maximum principal transmissivity, respectively. (B) Major structural controls are represented as a ternary system. The geometry and fault-zone deformation of major faults are major controls on flow in the Edwards Aquifer, as shown by the filled circle. Fault-block deformation is highly variable within the Edwards Aquifer and is best developed adjacent to mappable faults. Dashed arrow shows that an increasing role of fault-block deformation tends to place the aquifer nearer to the center of the ternary system.

Edwards Aquifer Authority, 2002, personal commun.). This observation warrants further structural and hydrologic investigations.

The Del Rio Formation introduces a very effective barrier to aquifer communication across faults, even in cases where fault displacement is greater than the thickness of the Del Rio Formation. The mechanically weak character of the clay-rich Del Rio Formation may allow it to smear along fault planes, resulting in a barrier to across-fault water movement. In the same way, shale of the Eagle Ford Formation is likely to remain an effective barrier to communication between the limestones of the Austin Group and the Buda Formation and Edwards Group limestones beneath.

In contrast, across-fault communication between the Edwards Group limestones and underlying limestones of the Glen Rose Formation is likely. Although argillaceous limestones are present intermittently in this stratigraphic section, there is no clay-rich shale separating the Edwards Group and Glen Rose Formation that would retard fault propagation as successfully as the Del Rio Formation. For this reason, the potential for aquifer communication between the Glen Rose Formation (Trinity Aquifer) and Edwards Aquifer warrants further analysis. This potential for flow communication is of great importance because the Glen Rose Formation crops out over a very large area adjacent to and north of the Edwards Aquifer recharge zone along the Balcones fault system. If water from the Glen Rose Formation feeds into the Edwards Aquifer along subsurface flow pathways, then the Edwards Aquifer recharge zone is in effect larger than currently described and modeled. Also, groundwater contamination north of the Edwards Aquifer recharge zone may be a threat to water quality in the Edwards Aquifer. Additional structural characterization, coupled with water-table characterization, pump testing, and natural and induced tracer tests, is needed to further evaluate the potential for subsurface aquifer communication.

SUMMARY

We investigated the geologic structure of the Edwards Aquifer to assess the large-scale aquifer architecture, analyze fault offset and stratigraphic juxtaposition relationships, evaluate fault-zone deformation and dissolution and fault-system architecture, and investigate fault-block deformation and scaling of small-scale (intrablock) normal faults. The goal was to assess the structural controls on the Edwards Aquifer at a broad range of scales that may influence water movement. At the largest scale, faults control the position and geometry of the recharge zone and confined zone and, combined with stratigraphy, define regional flow paths. At smaller scales, mappable fault zones themselves serve as recharge features and subsurface flow pathways. Fault displacements show a pattern of aquifer thinning that is likely to influence fault-block communication and flow paths. Flow-path constriction may be exacerbated by increased fault-segment connectivity associated with large displacements. Also, increased fault-zone deformation associated with larger-displacement faults is likely to further influence hydrologic properties. Smaller faults and fractures (sub–map scale) influence recharge and flow, but limited exposure of these features is not sufficient to perform systematic characterization.

Faulting over a range of scales is expected to produce strong permeability anisotropy such that maximum permeability is subhorizontal and parallel to fault-bedding intersections. Layer juxtaposition across faults allows the possibility of communication between the

Edwards Aquifer and permeable layers above and below the Edwards confining zones. This potential for communication could produce beneficial effects by enhancing recharge to the Edwards Aquifer and detrimental effects by enabling contaminant migration into the aquifer from a broader region. Fault-juxtaposition relationships alone do not adequately constrain the likelihood for across-fault fluid communication. The evaluation of fault-juxtaposition relationships should be coupled with analysis of fault-zone deformation processes in each mechanical layer and the relative likelihood of coating fault surfaces with impermeable fault rock (e.g., clay smear) that isolates permeable layers juxtaposed across faults. At all scales, we see indications that aquifer permeability will be relatively enhanced parallel to faults. Testing the role of these structural features with respect to hydrologic properties of the aquifer will require hydrologic testing tied to the geologic structure.

ACKNOWLEDGMENTS

This work was funded by the SwRI® (Southwest Research Institute) Internal Research and Development Program (project number R9223.01.001). Financial support for A. Schultz was provided by the San Antonio Water System. We thank Michelle Lee and Martin Marietta Materials for assistance and allowing us access for field work in the Beckmann Quarry. The San Antonio Water System, Bureau of Economic Geology, U.S. Geological Survey, and Edwards Aquifer Authority provided invaluable assistance. We especially thank Allan Clark, Eddie Collins, Sue Hovorka, Steve Johnson, Kirk Nixon, George Ozuna, Geary Schindel, and John Waugh for their assistance and suggestions during the course of this work. Mike Pittman (Area Manager) and Texas Parks and Wildlife, Black Gap Wildlife Management Area, kindly allowed us access to the Black Gap Wildlife Management area. Japan National Oil Corporation allowed us to use data we collected as part of work for them in 2000 and 2001. English Pearcy and Budhi Sagar improved this paper by their constructive reviews of the manuscript. Further detailed reviews by Stuart Rojstaczer and Brian McPherson considerably improved the manuscript. We appreciate the assistance of Rebecca Emmot and Sharon Odam in preparation of the manuscript.

REFERENCES CITED

Allan, U.S., 1989, Model for hydrocarbon migration and entrapment within faulted structures: American Association of Petroleum Geologists Bulletin, v. 73, p. 803–811.

Arnow, T., 1963, Ground-water geology of Bexar County, Texas: U.S. Geological Survey Water Supply Paper 1588, 36 p., 13 plates.

Barker, R.A., Bush, P.W., and Baker, E.T., Jr., 1994, Geologic history and hydrogeologic setting of the Edwards-Trinity Aquifer system, west-central Texas: U.S. Geological Survey Water-Resources Investigations Report 94–4039, 51 p.

Barnes, V.E., 1983, Geologic atlas of Texas, San Antonio sheet: Austin, University of Texas, Bureau of Economic Geology, 8 p., scale 1:250,000, 1 sheet.

Caine, J.S., Evans, J.P., and Forster, C.B., 1996, Fault zone architecture and permeability structure: Geology, v. 24, p. 1025–1028.

Clark, A.K., 2000, Vulnerability of ground water to contamination, Edwards Aquifer recharge zone, Bexar County, Texas, 1998: U.S. Geological Survey Water-Resources Investigations Report 00–4149, 9 p., 1 sheet.

Collins, E.W., 1993, Fracture zones between overlapping en echelon fault strands: Outcrop analogs within the Balcones fault zone, central Texas: Gulf Coast Association of Geological Societies Transactions, v. 43, p. 77–85.

Collins, E.W., 2000, Geologic map of the New Braunfels, Texas, 30 × 60 minute quadrangle: Geologic framework of an urban-growth corridor along the Edwards Aquifer, south-central Texas: Austin, University of Texas, Bureau of Economic Geology Miscellaneous Map 39, 28 p., 1:100,000 scale, 1 sheet.

Collins, E.W., and Hovorka, S.D., 1997, Structure map of the San Antonio segment of the Edwards Aquifer and Balcones fault zone, south-central Texas: Structural framework of a major limestone aquifer: Kinney, Uvalde, Medina, Bexar, Comal, and Hays Counties: Austin, University of Texas, Bureau of Economic Geology Miscellaneous Map 38, scale 1:250,000, 2 sheets.

Dawers, N.H., and Anders, M.H., 1995, Displacement-length scaling and fault linkage: Journal of Structural Geology, v. 17, p. 607–614.

Deike, R.G., 1990, Dolomite dissolution rates and possible Holocene dedolomitization of water-bearing units in the Edwards Aquifer, south-central Texas: Journal of Hydrology, v. 112, p. 335–373.

Dynamic Graphics, 2001, EarthVision User's Guide, Version 6.0, Alameda, California: Dynamic Graphics, Inc.

Ferrill, D.A., and Morris, A.P., 2001, Displacement gradient and deformation in normal fault systems: Journal of Structural Geology, v. 23, p. 619–638.

Ferrill, D.A., and Morris, A.P., 2003, Dilational normal faults: Journal of Structural Geology, v. 25, p. 183–196.

Ferrill, D.A., Stamatakos, J.A., and Sims, D.W., 1999a, Normal fault corrugation: Implications for growth and seismicity of active normal faults: Journal of Structural Geology, v. 21, p. 1027–1038.

Ferrill, D.A., Winterle, J., Wittmeyer, G., Sims, D.W., Colton, S., Armstrong, A., and Morris, A.P., 1999b, Stressed rock strains groundwater at Yucca Mountain, Nevada: GSA Today, v. 9, no. 5, p. 1–8.

Ferrill, D.A., Morris, A.P., Stamatakos, J.A., and Sims, D.W., 2000, Crossing conjugate normal faults: American Association of Petroleum Geologists Bulletin, v. 84, p. 1543–1559.

Finkbeiner, T., Barton, C.A., and Zoback, M.D., 1997, Relationships among in-situ stress, fractures and faults, and fluid flow: Monterey Formation, Santa Maria Basin, California: American Association of Petroleum Geologists Bulletin, v. 81, p. 1975–1999.

Foley, L.L., 1926, Mechanics of the Balcones and Mexia faulting: American Association of Petroleum Geologists Bulletin, v. 10, p. 1261–1269.

Groschen, G.E., 1996, Hydrogeologic factors that affect the flowpath of water in selected zones of the Edwards Aquifer, San Antonio region, Texas: U.S. Geological Survey Water-Resources Investigations Report 96–4046, 73 p.

Hanson, J.A., and Small, T.A., 1995, Geologic framework and hydrogeologic characteristics of the Edwards Aquifer outcrop, Hays County, Texas: U.S. Geological Survey Water-Resources Investigations Report 95–4265, 10 p.

Hovorka, S.D., Mace, R.E., and Collins, E.W., 1998, Permeability structure of the Edwards Aquifer, South Texas—Implications for aquifer management: Austin, University of Texas, Bureau of Economic Geology Report of Investigations 250, 55 p.

Kastning, E.H., 1981, Tectonism, fractures, and speleogenesis in the Edwards Plateau, central Texas, *in* Beck, B.F., ed., Eighth International Congress of Speleology, Bowling Green, Kentucky, July 18–24, 1981, Proceedings, Huntsville, Alabama: National Speleological Society Bulletin, v. 2, p. 692–695.

Loucks, R.G., 1999, Paleocave carbonate reservoirs: Origins, burial-depth modifications, spatial complexity, and reservoir implications: American Association of Petroleum Geologists Bulletin, v. 83, p. 1795–1834.

Maclay, R.W., 1989, Edwards Aquifer in San Antonio: Its hydrogeology and management: Bulletin of the South Texas Geological Society, v. 30, no. 4, p. 11–28.

Maclay, R.W., 1995, Geology and hydrology of the Edwards Aquifer in the San Antonio area, Texas: U.S. Geological Survey Water-Resources Investigations Report 95–4186, 64 p., 12 plates.

Maclay, R.W., and Rettman, P.L., 1972, Hydrologic investigations of the Edwards and associated limestones in the San Antonio area, Texas, Progress report, 1970–1971: U.S. Geological Survey Open-File Report 72–244, 24 p.

Maclay, R.W., and Small, T.A., 1976, Progress report on geology of the Edwards Aquifer, San Antonio area, Texas, and preliminary interpretation of borehole geophysical and laboratory data on carbonate rocks: U.S. Geological Survey Open-File Report 76–627, 65 p.

Maclay, R.W., and Small, T.A., 1983, Hydrostratigraphic subdivisions and fault barriers of the Edwards Aquifer, south-central Texas, USA: Journal of Hydrology, v. 61, p. 127–146.

Maclay, R.W., and Small, T.A., 1984, Carbonate geology and hydrology of the Edwards Aquifer in the San Antonio area, Texas: U.S. Geological Survey Open-File Report 83–537, 72 p., 14 sheets.

Maxwell, R.A., Lonsdale, J.T., Hazzard, R.T., and Wilson, J.A., 1967, Geology of the Big Bend National Park, Brewster County, Texas: The University of Texas at Austin, Bureau of Economic Geology Publication 6711, 320 p., 11 plates.

Mayer, J.R., and Sharp, J.M., Jr., 1998, Fracture control of regional ground-water flow in a carbonate aquifer in a semi-arid region: Geological Society of America Bulletin, v. 110, p. 269–283.

Morris, A.P., Ferrill, D.A., and Henderson, D.B., 1996, Slip-tendency analysis and fault reactivation: Geology, v. 24, p. 275–278.

Moustafa, A.R., 1988, Structural geology of Sierra del Carmen, Trans-Pecos Texas: Austin, University of Texas, Bureau of Economic Geology Geologic Quadrangle Map 54, 28 p., scale 1:48,000, 3 sheets.

Murray, G.E., 1956, Relationships of Paleozoic structures to large anomalies of coastal element of eastern North America: Gulf Coast Association of Geological Societies Transactions, v. 6, p. 13–24.

Murray, G.E., 1961, Geology of the Atlantic and Gulf Coastal province of North America: New York, Harper and Brothers, 692 p.

Palmer, A.N., 1991, Origin and morphology of limestone caves: Geological Society of America Bulletin, v. 103, p. 1–21.

Reeves, R.D., 1972, Maps showing outcrops of the Edwards and associated limestones in the principal recharge area of the Edwards Aquifer in Bexar County, Texas: U.S. Geological Survey Open-File Report 72–0310, 6 sheets.

Rose, P.R., 1972, Edwards Group, surface and subsurface, central Texas: Austin, University of Texas, Bureau of Economic Geology Report of Investigations 74, 198 p.

Sharp, J.M., Jr., and Banner, J.L., 1997, The Edwards Aquifer: A resource in conflict: GSA Today, v. 7, no. 8, p. 1–9.

Shaw, S.L., 1978, Structural geology of the Edwards Aquifer in the Castle Hills Quadrangle, northwestern San Antonio, Texas: Texas Journal of Science, v. 30, no. 2, p. 125–131.

Small, T.A., 1984, Identification and tabulation of geologic contacts in the Edwards Aquifer, San Antonio area, Texas: U.S. Geological Survey Open-File Report 84–075, 54 p.

Small, T.A., 1985, Identification and tabulation of geological contacts in the Edwards Aquifer, San Antonio area, Texas: Texas Department of Water-Resources Report LP-199, 54 p.

Small, T.A., and Hanson, J.A., 1994, Geologic framework

and hydrogeologic characteristics of the Edwards Aquifer outcrop, Comal County, Texas: U.S. Geological Survey Water-Resources Investigations Report 94–4117, p.10, 1:75,000 scale, 1 plate.

Southwest Research Institute (SwRI), 2000, 3DStress user's guide, Version 1.3.3: San Antonio, Texas, Southwest Research Institute.

Stein, W.G., and Ozuna, G.B., 1996, Geological framework and hydrogeologic characteristics of the Edwards Aquifer recharge zone, Bexar County, Texas: U.S. Geological Survey Water-Resources Investigations Report 95–4030, p. 8, 1:75,000 scale, 1 plate.

Walsh, J.J., and Watterson, J., 1988, Dips of normal faults in British Coal Measures and other sedimentary sequences: Geological Society [London] Journal, v. 145, p. 859–873.

Weeks, A.W., 1945, Balcones, Luling, and Mexica fault zones in Texas: American Association of Petroleum Geologists Bulletin, v. 29, p. 1733–1737.

Wermund, E.G., and Cepeda, J.C., 1977, Regional relation of fracture zones to the Edwards Limestone Aquifer, Texas, *in* Tolson, J.S., and Doyle, F.L., eds., Proceedings of the Twelfth International Congress on Karst Hydrogeology: Huntsville, Alabama, University of Alabama in Huntsville Press, p. 239–253.

Wermund, E.G., Joseph, C.C., and Luttrell, P.E., 1978, Regional distribution of fractures in the southern Edwards Plateau and their relationship to tectonics and caves: Austin, University of Texas, Bureau of Economic Geology Geological Circular 78–2, 14 p.

Withjack, M.O., Olson, J., and Peterson, E., 1990, Experimental models of extensional forced folds: American Association of Petroleum Geologists Bulletin, v. 74, p. 1038–1054.

Young, K., 1972, Mesozoic history, Llano region, *in* Barnes, V.E., Bell, W.C., Clabaugh, S.E., Cloud, P.E., Jr., McGehee, R.V., Rodda, P.U., and Young, K., eds., Geology of the Llano region and Austin area, field excursion: Austin, University of Texas, Bureau of Economic Geology Guidebook 13, 154 p.

MANUSCRIPT RECEIVED BY THE SOCIETY 9 MAY 2002
REVISED MANUSCRIPT RECEIVED 21 JULY 2003
MANUSCRIPT ACCEPTED 31 JULY 2003

Printed in the USA